

Self-Powered Sensor for Quantifying Ocean Surface Water Waves Based on Triboelectric Nanogenerator

Chuguo Zhang,[†] Lu Liu,[†] Linglin Zhou,[†] Xing Yin, Xuelian Wei, Yuexiao Hu, Yuebo Liu, Shengyang Chen, Jie Wang,* and Zhong Lin Wang*

Cite This: *ACS Nano* 2020, 14, 7092–7100

Read Online

ACCESS |

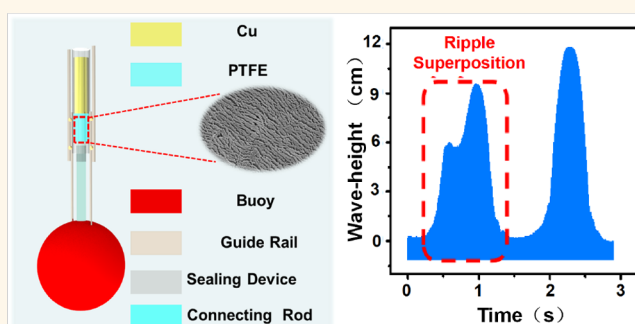
Metrics & More

Article Recommendations

Supporting Information

ABSTRACT: An ocean wave contains various marine information, but it is generally difficult to obtain the high-precision quantification to meet the needs of ocean development and utilization. Here, we report a self-powered and high-performance triboelectric ocean-wave spectrum sensor (TOSS) fabricated using a tubular triboelectric nanogenerator (TENG) and hollow ball buoy, which not only can adapt to the measurement of ocean surface water waves in any direction but also can eliminate the influence of seawater on the performance of the sensor. Based on the high-sensitivity advantage of TENG, an ultrahigh sensitivity of 2530 mV mm^{-1} (which is 100 times higher than that of previous work) and a minimal monitoring error of 0.1% are achieved in monitoring wave height and wave period, respectively. Importantly, six basic ocean-wave parameters (wave height, wave period, wave frequency, wave velocity, wavelength, and wave steepness), wave velocity spectrum, and mechanical energy spectrum have been derived by the electrical signals of TOSS. Our finding not only can provide ocean-wave parameters but also can offer significant and accurate data support for cloud computing of ocean big data.

KEYWORDS: triboelectric nanogenerator, high performance, ocean wave spectrum, wave energy, self-powered, sensor



Ocean waves, as the main component of motion in the ocean, have a close relationship with wind, submarine topography, planetary gravitation, and marine disasters, and its research plays a vital role in the blue energy harvesting, weather forecast, marine resources development, and early warning of natural disasters.^{1–7} It is self-evident that the extraction of high-precision ocean-wave spectrum information is crucial in the research of ocean water waves. Consequently, various ocean-wave spectrum sensors have been designed for the demand of accurate ocean-wave spectrum detection, such as radar remote sensing, photoelectric remote sensing, and capacitance-based liquid level sensor.^{8–11} However, some important reasons limit the applications of above sensors in the progress of high-precision ocean-wave spectrum detection. As for monitoring an ocean-wave spectrum by using radar remote sensing and photoelectric remote sensing technologies, which are based on the recurrent inversions and Fourier transforms of first signals, it is difficult to meet the requirement of high precision because of the serious signal distortion during the signal processing.¹² Meanwhile the special requirement of aerospace platform

limits their real-time acquisition of ocean-wave spectra.^{9,13,14} On the other hand, although capacitance-based liquid level sensors exhibit excellent detection performance in ocean-wave spectra, the extreme marine environment (the high-corrosion and rapid composition changes of seawater) makes their practicability substantially decline in the real marine environment. In particular, external energy storage devices such as batteries are always required for these sensors to monitor ocean-wave spectra, which limited lifetime, non-negligible replacement costs, and environmental issues greatly limit their application.

Recently, triboelectric nanogenerators (TENGs), based on the principle of triboelectrification effects and electrostatic

Received: March 2, 2020

Accepted: June 5, 2020

Published: June 5, 2020



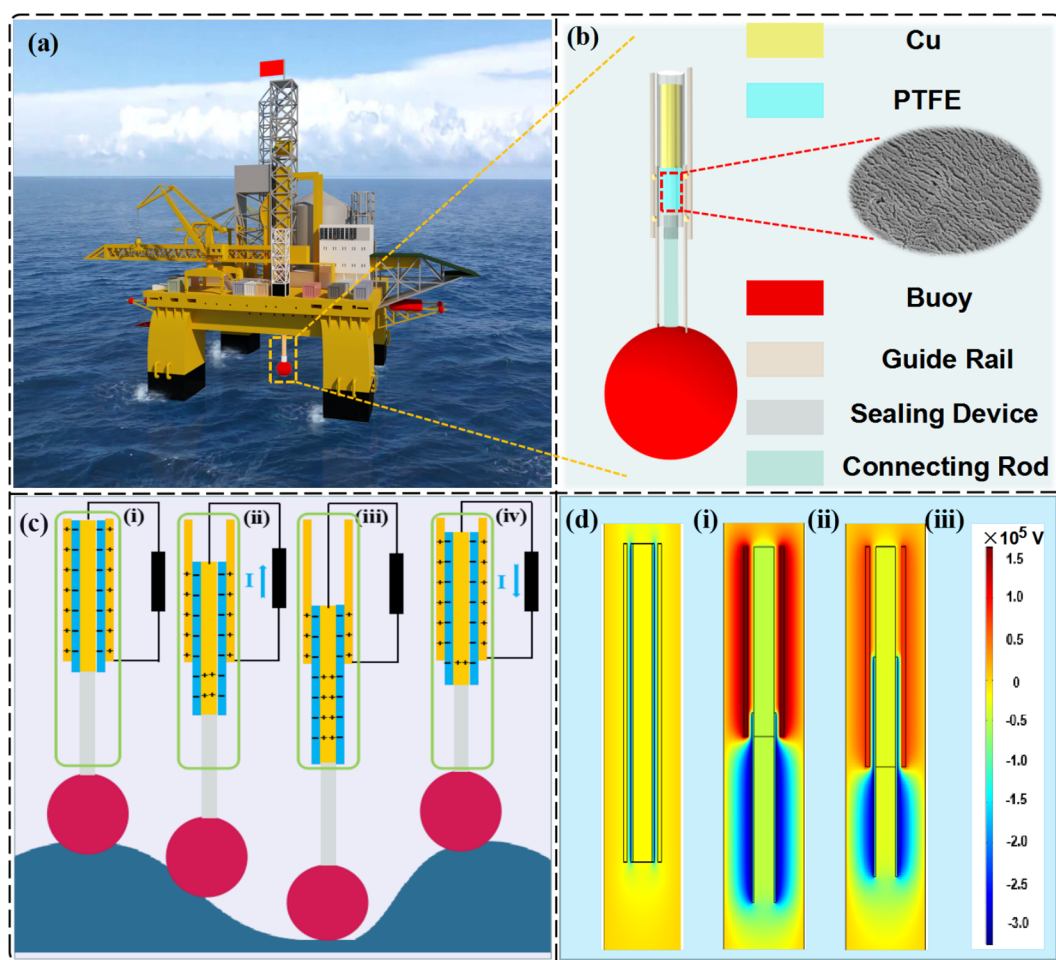


Figure 1. Structural design and working mechanism of the TOSS. (a) Schematic diagram of the fabricated TOSS with an offshore drilling platform. (b) Detailed structure of TOSS. The inset picture is the SEM image of the PTFE surface. (c) Working principle of the sensor device. (d) COMSOL simulation of the voltage potential distribution of the TOSS under different state.

induction,^{14,15,16} have been developed to convert mechanical energy into electrical energy.^{17–20} Due to the low cost, low weight, and high sensitivity, and high efficiency in low frequency, TENGs have been widely used in both energy harvesting and self-powered sensing.^{20–26} Very recently, a liquid–solid contact TENG (LC-TENG) was designed for monitoring wave height, which exhibited a high sensitivity in the sodium chloride solution.²⁷ With the advantages of self-power and high sensitivity,²⁸ an ocean-wave spectrum sensor based on TENG may be considered as the next-generation ocean-wave spectrum sensor instead of conventional ocean-wave spectrum sensors. However, single-parameter measurement and environmental vulnerability are the main challenges for the application of LC-TENG. Therefore, further development of water wave spectrum sensors based on TENG should be design to satisfy the requirements of multiparameter detection including wave height (H), wave period (T), wave frequency (f), wave velocity (v), wavelength (L), wave steepness (δ), ocean-wave velocity spectrum, kinetic energy spectrum, and eliminating the impact of harsh environment in the real seawater.

In this work, a hollow-ball buoy-assisted triboelectric ocean-wave spectrum sensor (TOSS), based on the sliding mode tubular TENG, is designed as an high-performance and self-powered ocean-wave spectrum sensor. By using a hollow-ball buoy as an auxiliary device and a tubular TENG as an ocean-

wave spectrum sensor, this design can eliminate the influence of seawater on the performance of the sensor and realize the monitoring of ocean-wave spectrum in an arbitrary direction with an ultrahigh sensitivity of 2530 mV mm^{-1} (which is 100 times higher than that of the previous work) and a minimal monitoring error of 0.1% in the detection of wave height and wave period, respectively. In addition, based on the high-sensitivity characteristic of TOSS, multiparameters H , T , f , v , L , and δ of ocean waves can be monitored in real-time. Furthermore, the ocean-wave velocity spectrum and ocean-wave mechanical energy spectrum can be extracted from the output performance of TOSS for guiding future and more efficient wave energy harvesting devices structural design. Owing to the capability of directly converting the mechanical signal of ocean-wave into the electrical signal for TOSS, the active ocean-wave sensing without an additional power source can be realized. Based on the excellent performance of TOSS, it will play a vital role in a great deal of marine research in the future.

RESULTS AND DISCUSSION

Structure Design and Working Principle. As a type of ocean-wave spectrum sensor, TOSS can be combined with various existing ocean equipment such as an offshore drilling platform to monitor the ocean-wave information. As illustrated in Figure 1a, it can be assembled into an offshore drilling

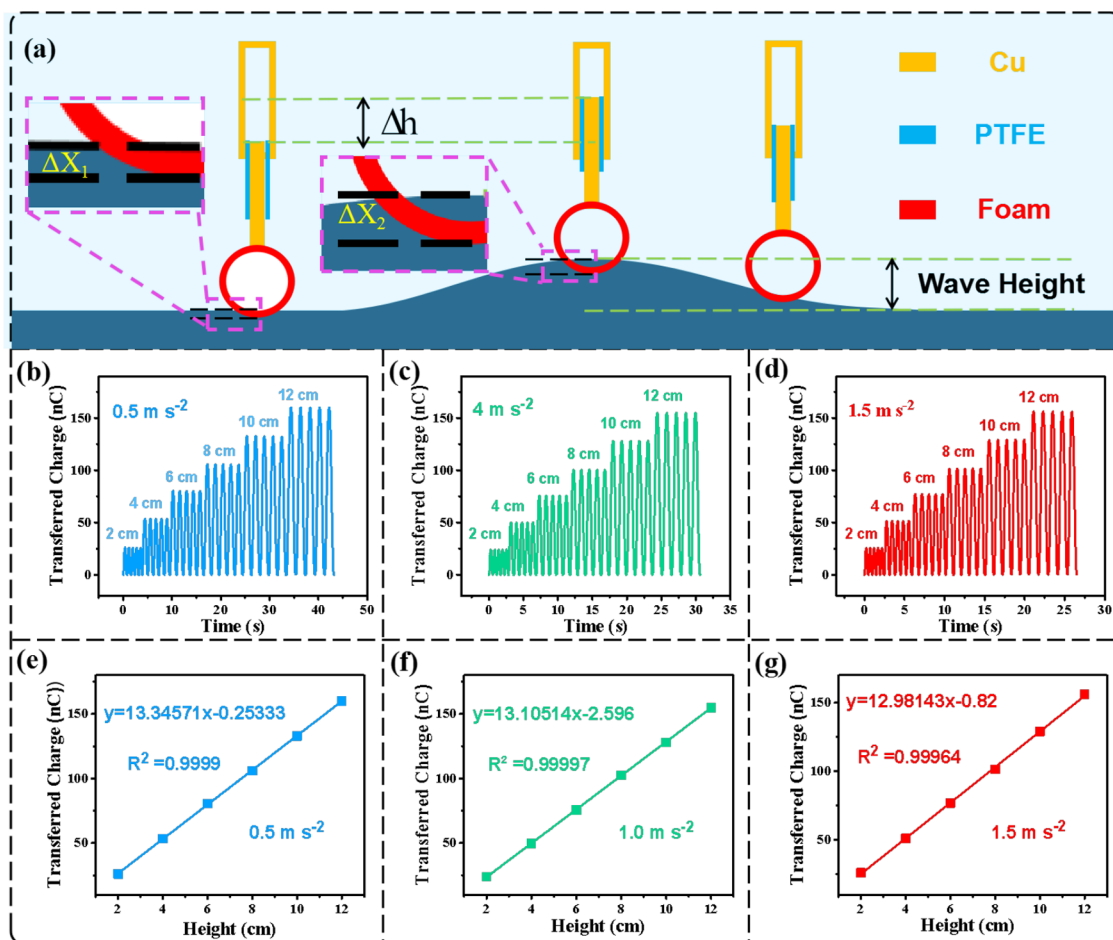


Figure 2. Characterization of wave height the TOSS. (a) Working principle of measuring wave height with the TOSS. (b–d) Transferred charges of TOSS at the different wave heights and various accelerations. (e–g) Wave height linear relationship of TOSS with the different accelerations.

platform as an ocean-wave spectrum sensor to convert the wave energy into electricity, where the information on ocean-wave spectra can be extracted from the output signal. Figure 1b displays the detailed structure of TOSS, which consists of two copper tubes with different diameters as external and inner electrodes (one has an inner diameter of 10 mm and the other has an outer diameter of 9.5 mm) and a polytetrafluoroethylene (PTFE) film with a thickness of $200 \mu\text{m}$ as the dielectric layer stuck to the inner electrode. Meanwhile, the whole sensor device contains a hollow-ball foam buoy (HFB) with a diameter of 15 cm, which is applied to drive the TOSS with rocking on the waves and reduces the contact probability between the TOSS and seawater for eliminating the influence of seawater on the output performance. Besides, the design of the connecting rod and sealing device can ensure that the performance of TOSS is not affected by the external environment, and the guide rail can improve the output performance, stability, and service life of the TOSS. Based on the structural design of HFB and tubular TENG, the measurement of ocean waves in any direction can be guaranteed. A scanning electron microscopy (SEM) image of the PTFE film surface reveals the micronanostructure to obtain a larger signal output (see the enlarged figure in the Figure 1b). The working principle of the TOSS is displayed in Figure 1c. In the original state, the external copper and dielectric layer will contact each other when the HFB floats in a crest,

resulting in negative charges on PTFE surface and positive charges on the external electrode because of the tribo-electrification (Figure 1c(i)). Once they are separated by the waves, the potential difference between the two electrodes will be produced, which will drive electrons to flow from the inner electrode to the external electrode, generating a pulse current in the external circuit (Figure 1c(ii)). The maximum output will be obtained when the two electrodes are completely separated (Figure 1c(iii)). When the other wave spreads to directly below the HFB, the HFB will raise up with the wave, thereby the dielectric layer will return back to the original position, resulting in a reversed current flow to balance the potential difference (Figure 1c(iv)). Therefore, the mechanical energy of an ocean-wave motion is transformed into the electric energy, while the ocean-wave spectrum can be extracted by the output signal of the TOSS. To better understand the output performance of the TOSS, the potential distribution on the two electrodes at different states was simulated by using the finite element analysis method (COMSOL Multiphysics), respectively (Figure 1d). When the sliding separation distance of TOSS is 10 cm, the open-circuit voltage of it can reach $3 \times 10^5 \text{ V}$.

Wave Height Sensing of TOSS. As for ocean-wave spectrum sensing, the wave height is a crucial evaluation standard for the TOSS. Therefore, in order to characterize the detective performance of the TOSS for wave height, a linear

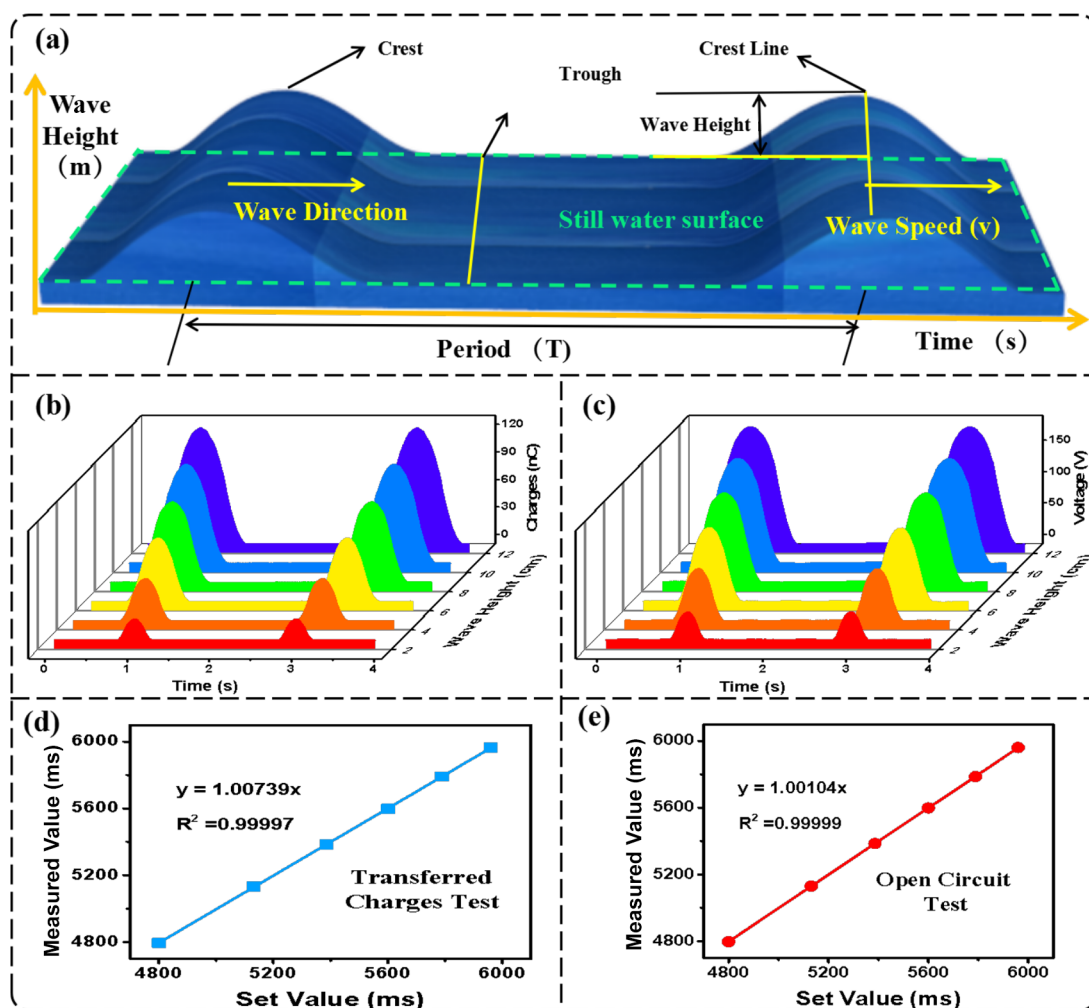


Figure 3. Extracting ocean-wave spectra from the output signals of TOSS. (a) The ideal structure and characteristic parameters of an ocean-wave spectrum. (b) and (c) The different wave height and period of ocean-wave spectra through transferred charges and open-circuit voltage. (d) and (e) The relationship between the theoretical value of wave period and the measured value extracting from the transferred charges signal and open-circuit voltage signals of TOSS.

motor is utilized to simulate various wave heights. As presented in Figure 2a, the moving distance of TOSS, which decides the output performance, closely equals the wave height. Therefore, the wave height can be extracted from the output signal of the TOSS, achieving the wave height sensing. It is worth mentioning that the effect of friction induced by a sliding mode can be greatly reduced by using PTFE with a small coefficient (about 0.04) (inset image in Figure 2a, Figure S1 and Supplementary Note 1). To investigate the performance of the TOSS in wave height detection, we applied a vertical linear motor as an external drive, which provides a precise and various movement pattern in the vertical direction. The displacement of a motor reciprocating motion ranging from 2 to 12 cm with an interval of 2 cm at different accelerations (0.5 m s^{-2} , 1.0 m s^{-2} , 1.5 m s^{-2}) is used to simulate the ocean waves at different wave heights, respectively. The corresponding transferred charges of TOSS are presented in Figure 2b–d. At different accelerations, the transferred charges increase with the displacement from 25 nC at 2 cm to 160 nC at 12 cm. Meanwhile, the open-circuit voltage rises with the displacement increasing from 27 V at 2 cm to 280 V at 12 cm (Figure S2a–c). Notably, the corresponding output of the TOSS is only related to the displacement of the motor and not to the

acceleration. The result is in accordance with the proposed measuring mechanism in Figure 2a, which is an important foundation for wave height detection (Supplementary Note 2). In addition, both transferred charges and open circuit exhibit excellent linearity with the displacement of the motor with high correlation coefficients of 0.99994 and 0.9977, respectively (Figure 2e,f and Figure S3a–c). The ultrahigh linearity between the output performances of TOSS and the simulating wave height enables it to be a sensitive wave-height sensor. Due to the contact sliding between dielectric layer and copper electrode (solid–solid sliding mode) without the effect of a salt solution and the rigorous mathematical geometric structure design, the TOSS has achieved a high sensitivity of 2530 mV mm^{-1} (Figure S4 and Supplementary Note 3), which is 100 times higher than that of LS-TENG sensor (23.5 mV mm^{-1}).²⁷ These results indicate that the TOSS has the capability for detecting waves with a smaller size and higher accuracy. In addition, the TOSS also can be used as a generator to convert wave energy into electrical energy. To investigate the capability of harvesting wave energy, the TOSS is used as a power source to charge a capacitor ($1 \mu\text{F}$). It can take 30 s to charge a capacitor ($1 \mu\text{F}$) from 0 to 2.9 V at 0.5 m s^{-2} , 3.9 V at 1.0 m s^{-2} , and 4.7 V at 1.5 m s^{-2} , respectively (Figure S5).

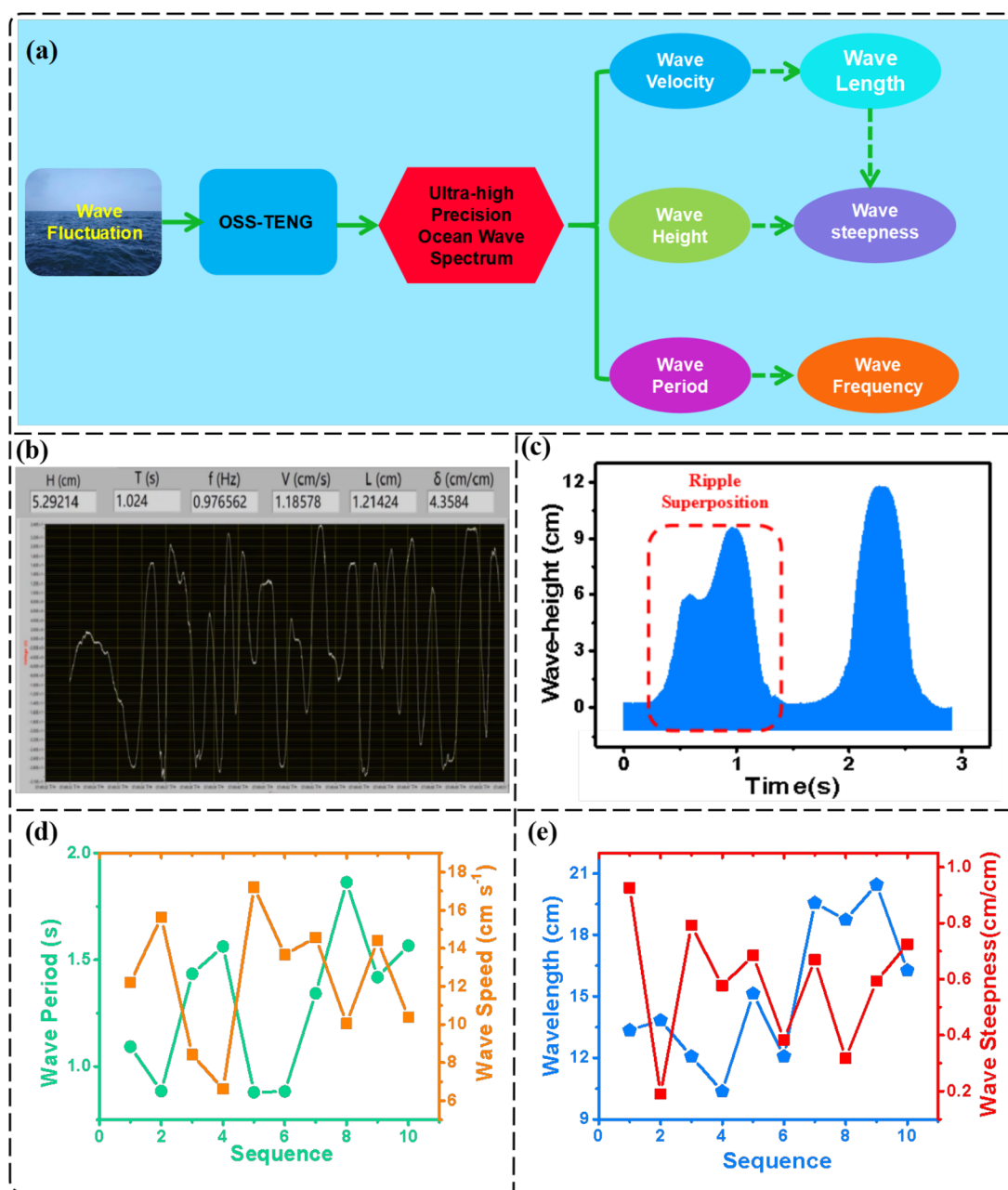


Figure 4. Measurement and application of TOSS in simulated water waves. (a) The flowchart for acquisition of an ocean-wave spectrum and multiparameters of an ocean wave. (b) The six parameters real-time display of TOSS with the simulated water wave. (c) The water wave height spectrum extracting from transferred charges of the TOSS. (d) The real-time monitoring change of wave period and wave velocity of a water wave. (e) The real-time monitoring change of wavelength and wave steepness of a water wave.

Importantly, it is obvious that the output performance of the TOSS is basically unchanged after 1000 test cycles, which proves the high stability of TOSS (Figure S6).

Sensing Performance of TOSS for the Simulated Ocean-Wave Spectrum. Although the real ocean-wave spectrum is generally displayed as the relationship between wave height and position ($H-s$), we can obtain the real ocean-wave spectrum by using the TOSS to extract the ocean-wave relation spectrum between wave height and time ($H-t$) at one point. Because the horizontal spread speed of waves at a certain area of the sea can simply be regarded as a fixed value in motion and ocean-wave spectrum, research can focus on the wave motion in the vertical direction.²⁹ Therefore, based on the propagation velocity (v) of waves, we can easily transform

the signal spectrum obtained by the TOSS ($H-t$) into the real ocean-wave spectrum ($H-s$) through the relationship among $s-v-t$. In summary, a vertical linear motor was used to simulate the real ocean-waves motion and investigate the performance of TOSS. The ideal ocean-wave spectrum contains many parameters and information on ocean waves, such as H , T , f , v , L , δ , and spread direction (Figure 3a), which are important for ocean investigation. First of all, the sensing performance of the TOSS is evaluated by comparing the motion spectrum with the actual spectrum of the motor motion. The theoretical analysis diagrams of physical motion models and the ideal scanning signal images of the TOSS are displayed in Figures S7 and S8 and Supplementary Note 4. At the same time, the real extraction spectra of TOSS are shown

in Figure S9a–c. It clearly shows that the testing charts of TOSS are exactly similar to the ideal images, indicating that the TOSS can be used as a high-performance ocean-wave spectrum sensor. In order to fully test the performance of the TOSS for detecting various ocean-wave spectra, we add a pause in the vertical motor test to simulate the motion state in a still water surface. Figure 3b,c depicts various ocean-wave spectrum signals with the different wave heights ranging from 2 to 12 cm and wave period by extracting the transferred charges signal and open-circuit voltage signal of TOSS. The characteristics of these spectrum signals are basically the same as ideal ocean spectrum signals in Figure 3a, which verify the excellent detection performance of the TOSS again. In addition, the wave-period (T) has a close relationship with the major natural disasters in oceans, such as a submarine earthquake and hurricane, so it is crucial for us to obtain a high-precision wave period for the research and forecast of marine natural disasters. Meanwhile, the transferred charges and open-circuit voltage signals of TOSS contain the wave period information on ocean waves, and the relationship of between the theoretical value of the wave period and the measured value with the transferred charges signal and open-circuit voltage signals of TOSS are presented in Figure 3d,e, respectively. It is obviously clear that the linear correlation coefficient can achieve 0.99997 and the linear slope can realize 1.00104, which display the ultrahigh sensitivity of the TOSS for the wave period. Besides, it is also noteworthy that the TOSS can easily achieve a monitoring of millisecond level and a monitoring error of 0.1% in the period measure of ocean waves (Supplementary Tables 1–2 and Supplementary Note 5). If the wave period is extracted, we can easily obtain the wave frequency of ocean waves by the formula of the relationship between frequency and period. More importantly, according the high-precision ocean-wave spectrum detected by the TOSS and the related geometric size parameters of it, we can obtain the wave velocity, wavelength, and wave steepness of ocean waves. The corresponding theories and computation process are shown in Figure S10 and Supplementary Note 6. Therefore, we can continuously scan the ocean-wave spectrum, achieving the detection of H , T , f , v , L , and δ of ocean waves. Simultaneously, for the advantages of low-price and simple structure and the numerous sensors based on TOSS that conveniently form a network for scanning the ocean-wave spectra in a specific sea area, we will obtain more characteristic information on ocean waves, for example, spread direction, and the coordination errors are greatly eliminated (Figure S11 and Supplementary Note 7).

Detection Performance of TOSS in Water Waves. To analyze the performance of TOSS on a real ocean-wave spectrum, it is tested in a water tank to simulate the motion of ocean waves. Figure 4a displays the detailed flowchart of an ocean-wave spectrum and the acquisition of ocean-wave parameters. As is shown in Video S1 and Figure 4b, the TOSS can directly detect the high-precision water wave spectrum and real-time monitor the multiparameters of the water wave, including H , T , f , v , L , and δ . Although the real sea surface includes many tiny ripples and a few ocean waves are different from the uniform ripples produced, the perfect detection performance of TOSS for ripples is displayed in this work. In addition, it is well known that the wave height of ocean waves is higher than that of ripples. Therefore, we can add a filter program to the sensing software to obtain a digital ocean-wave spectrum, which only includes high-precision ocean wave information, by eliminating the small ripple spectrum signal,

and then achieve the multifunction of TOSS in the real ocean-wave monitoring. Meanwhile, the TOSS can directly convert the mechanical signal of the ocean wave into the electrical signal even in low frequency, realizing a self-powered ocean-wave sensing without an additional power source. For example, a green LEDs bulb array (rated power 45 mW \times 12) can also be lit up by a TOSS, which can harvest wave energy (Video S2). For converting the mechanical energy of periodic water wave vibration into the pulse alternating current output by the TOSS, the LEDs array flicker alternately, and the circuit diagram is presented in Figure S12. Therefore, in practical applications, a real-time and completely self-powered ocean-wave spectrum monitoring system can be achieved by harvesting wave energy *in situ* through integrating the TOSS with other technologies and then solve the dependence of existing sensors on batteries. Figure 4c and Figure S13 depict the real water wave height spectrum scanned by the transferred charges and open-circuit voltage signals of TOSS, respectively. It is clearly found that they are basically the same as the water-wave spectrum, and the superimposed signals of multiple waves are clearly visible (Figure 3a). In addition, the kinetic energy and velocity of an ocean wave can be decomposed in the vertical direction and in the propagation direction (Figure S14). First, there is a direct linear relationship between the transferred charges of TOSS (or open-circuit voltage) and the quadratic of the wave velocity in the vertical direction, respectively (Supplementary Note 4). Since the projection area of the surface contacted by hollow buoy and seawater on the horizontal plane (which is a circle with a radius of R) remains unchanged (Figure S15), the kinetic energy spectrum of an ocean wave in the vertical direction (E_{kv}) can be obtained by the following equation (Supplementary Note 8):

$$E_{kv}(t) = a_v \rho_s v R W \{ \Delta Q(t) \}^2 / 2\pi \sigma^2 D^2 \quad (1)$$

$$E_{kv}(t) = a_v \rho_s v R W \{ V(t) \}^2 / 2\pi k^2 \sigma^2 D^2 \quad (2)$$

where a_v is the obtained acceleration of an ocean wave in the vertical direction by TOSS (a_v is basically a fixed constant), ρ_s is the density of seawater, v is the wave-velocity by TOSS, R is the projection radius of the surface contacted by a hollow buoy and seawater on the horizontal plane, W is the transverse width of ocean-wave, $\Delta Q(t)$ is the transferred charge spectrum of TOSS, $V(t)$ is the open-circuit voltage spectrum of TOSS, k is the relevant scale factor of V and wave-height (H), σ is the surface charge density of PTFE, and D is the diameter of PTFE. Based on the transferred charge spectrum (or open-circuit voltage spectrum) and wave-velocity extracted by TOSS, we can get the true ocean-wave shape spectrum and then achieve the kinetic energy spectrum of an ocean wave in the propagation direction (E_{kp}) by the following eqs (Supplementary Note 9).

$$E_{kp}(t) = \rho_s v^3 R W \Delta Q(t) / 4\sigma D \quad (3)$$

$$E_{kp}(t) = \rho_s v^3 R W V(t) / 4k\sigma D \quad (4)$$

Meanwhile, we can also obtain the gravitational potential energy spectrum of an ocean wave (E_p) by the following eqs 5 or 6 (Figure S16 and Supplementary Note 10):

$$E_p(t) = \rho_s g v^2 R W \{ \Delta Q(t) \}^2 / 4\pi \sigma^2 D^2 \quad (5)$$

$$E_p(t) = \rho_s g v^2 R W \{ V(t) \}^2 / 4\pi k^2 \sigma^2 D^2 \quad (6)$$

where g is the gravitational acceleration. Therefore, we can easily get the mechanical energy spectrum of an ocean wave by simply adding the kinetic energy spectrum of the ocean wave in the vertical and propagation directions and the gravitational potential energy of an ocean wave (which is based on the eqs 7 or 8).

$$E_m(t) = a_v \rho_s v RW \{ \Delta Q(t) \}^2 / 2\pi \sigma^2 D^2 + \rho_s v^3 RW \Delta Q(t) / 4\sigma D + \rho_s g v^2 RW \{ \Delta Q(t) \}^2 / 4\pi \sigma D^2 \quad (7)$$

$$E_m(t) = a_v \rho_s v RW \{ V(t) \}^2 / 2\pi k^2 \sigma^2 D^2 + \rho_s v^3 RW V(t) / 4k\sigma D + \rho_s g v^2 RW \{ V(t) \}^2 / 4\pi k^2 \sigma^2 D^2 \quad (8)$$

where $E_m(t)$ is the mechanical energy spectrum of an ocean wave. Therefore, it is easy to obtain the mechanical energy of a single ocean wave (E) through the following integral formula 9 or 10:

$$E = \int_{t_1}^{t_2} \left(\frac{2a_v \rho_s v RW + \rho_s g v^2 RW}{4\pi \sigma^2 D^2} \right) \{ \Delta Q(t) \}^2 dt + \int_{t_1}^{t_2} \frac{\rho_s v^3 RW}{4\sigma D} \Delta Q(t) dt \quad (9)$$

$$E = \int_{t_1}^{t_2} \left(\frac{2a_v \rho_s v RW + \rho_s g v^2 RW}{4\pi k^2 \sigma^2 D^2} \right) \{ V(t) \}^2 dt + \int_{t_1}^{t_2} \frac{\rho_s v^3 RW}{4k\sigma D} V(t) dt \quad (10)$$

where t_1 is the time that the ocean wave first acts on the TOSS and t_2 is the time the ocean wave leaves the TOSS. Compared with the classical formula for the calculation of ocean-wave energy ($P = a\rho g^2 TH^2$, where P is the energy of an 1 m wide ocean wave, a is proportionality coefficient, ρ is the density of seawater, g is the acceleration of gravity, T is the period of an ocean wave, and H is the wave height of an ocean wave), it is not difficult to find that this work is about the calculation of the total mechanical energy of ocean waves, which not only includes the kinetic energy and gravitational potential energy of an ocean wave in the vertical direction but also includes the kinetic energy of an ocean wave in the horizontal direction. Therefore, compared with the classical method, this work can improve the calculation accuracy of ocean wave energy. On the other hand, the velocity spectrum of an ocean wave in the vertical direction ($v_v(t)$) has a quadratic relationship with the short-circuit current of TOSS (Supplementary Note 8):

$$v_v(t) = 2I(t) / \pi \sigma d \quad (11)$$

where $I(t)$ is the short-circuit current spectrum of the TOSS. So we can easily extract the velocity spectrum of an ocean wave in the vertical direction through the short-circuit current signal of it (Figure S17). Meanwhile, we can get the velocity spectrum of an ocean wave by the vector superposition of the velocity spectrum of an ocean wave in the vertical direction and propagation velocity, which are obtained by the TOSS. Therefore, the three kinds of spectra by TOSS will largely facilitate the study of velocity and energy distribution of ocean waves, so as to provide sufficient data support for how to more efficiently harvest the wave energy in different sea areas. Although a single TOSS can only obtain the two-dimensional velocity and kinetic energy distribution of ocean waves, the three-dimensional or even a large range of velocity and kinetic energy distribution of ocean waves also can be extracted by multiple TOSS networks integrated with computer technology to better serve the research of the ocean and the harvesting of blue energy in the future. In addition, the design of a

cylindrical TOSS and spherical buoy exhibits excellent stability on monitoring the wave spectrum in any direction. By the real-time monitoring changes of wave period, wave velocity, wavelength, and wave steepness of a water wave are depicted in Figure 4d,e, we can find that the wave period and wave velocity show an opposite change trend in the range of 0.9–2.8 s and 6–18 cm s⁻¹, respectively. In addition, we can also observe the fluctuation of wavelength and wave steepness in the range of 10–20 and 0.2–1.0 cm/cm, respectively.

CONCLUSION

In a summary, we reported a self-powered and high-performance triboelectric ocean-wave spectrum sensor (TOSS) fabricated using a tubular triboelectric nanogenerator (TENG) and hollow-ball buoy, which not only can adapt to the measurement of ocean waves in any direction but also can eliminate the influence of seawater on the performance of the sensor. Based on the excellent sensing performance of TOSS, an ultrahigh sensitivity of 2530 mV mm⁻¹ (which is 100 times higher than that of previous work) and a minimal monitoring error of 0.1% are achieved in the testing of wave height and wave period, respectively. Meanwhile, the TOSS has the function of real-time monitoring the wave height (H), period (T), frequency (f), wave velocity (v), wavelength (L), and wave steepness (δ) of ocean-wave by obtaining the high-precision ocean-wave spectrum and the design parameters of the TOSS. Furthermore, the velocity and mechanical energy spectrum of an ocean wave, which provides a vital theoretical basis for the design of advanced and more efficient wave energy harvesting devices, can be obtained by the electrical signals of the TOSS. On the basis of this property, we propose an ocean-wave spectrometer based on the TENG technique, which can simplify the signal processing circuit and reduce the power consumption. More importantly, it also has a huge potential to realize a complete self-powered ocean-wave spectrum by harvesting wave energy *in situ* and combining it with the energy management and storage modules, solving the common problem of battery dependence of the existing ocean sensors. Besides, due to the low price and simple structure of the sensor, the large-scale sensors array can be used to detect the ocean-wave spectrum in a wide range of sea areas and then obtain more parameters of the waves and the detailed hydrological characteristic of the sea areas. As a result, this ocean sensor may play a crucial role in ocean-wave research, marine geological survey, and other research areas and then greatly accelerate the pace of human exploration and understanding of the ocean in the future.

METHODS

Fabrication of the TOSS. A PTFE film (25 cm × 2.7 cm × 200 μm) was wrapped with copper tube (outside diameter 9.5 mm and length 30 cm) by double-sided tape (50 μm), and the other copper tube (internal diameter 10 mm) was selected as a triboelectric electrode. In addition, a spherical foam of 15 cm diameter was applied as a buoy, which can drive the internal triboelectric electrode to move. Meanwhile, a 5 mm thickness acrylic board obtained the modules of specific shape by using a laser cutting machine and then spliced into the corresponding test brackets by glue, which is shown in Figure 2a. Subsequently, a 10 mm thickness acrylic board is cut into many circular structures with different hole diameters (5 and 1 cm) to fix the TOSS in the test of water waves. Finally, the camera tripod, the above circular structure with hole, and TOSS are glued together to form the relevant testing structure by hot melt glue.

Detective Measurement of the TOSS. To fully simulate the wave motion, a vertical linear motor (PS01-37S ×120F-HP-N) was applied to drive the TOSS with different parameters. A water tank (2.7 m × 0.7 m × 0.7 m) was used to simulate the ocean waves. The programmable electrometer (Keithley model 6514) was utilized to monitor the transferred charges, open-circuit voltage, and short-circuit current. A potentiostat (Biologic, VMP3) was adopted to extract the voltage signal of the capacitor in a self-powered system. An electronic watch is measured to form a self-driven data progressing system.

ASSOCIATED CONTENT

Supporting Information

The Supporting Information is available free of charge at <https://pubs.acs.org/doi/10.1021/acsnano.0c01827>.

Video S1: The six parameters real-time display of TOSS with the simulated water wave (MP4)

Video S2: The LED array is lighted by TOSS in a water wave (MP4)

Supporting Notes 1–10 provide the error analysis of wave height measured by TOSS; the principle and relationship of wave height by TOSS; the relationship of TOSS structure design; the theoretical motion model of motor motion and the measurement principle of TOSS; the description of relevant letter parameters in the TOSS error analysis table; the principle of wave frequency, wave velocity, wavelength and wave steepness with TOSS; the principle ocean-wave propagation direction measurement with TOSS network; the principle of measuring the kinetic energy of ocean waves in the vertical direction with TOSS; the principle of measuring the kinetic energy of ocean waves in the propagation direction with TOSS; the principle of measuring the gravitational potential energy of ocean waves in the propagation direction with TOSS. Figures S1–S16 provide the error analysis of wave height measurement by the TOSS; the open-circuit voltage of TOSS at the different wave heights and various acceleration; the linear relationship between wave height and the open-circuit voltage signals of TOSS under the different acceleration; the geometric design of TOSS; the charging-capacitor curve of TOSS under different acceleration; the test of the stability of TOSS by linear motor; the physical motion mode of vertical linear motor; the ideal signal spectra of TOSS; the real obtained spectra by TOSS; the analysis of ocean spectral structure obtained by the TOSS; the principle of detecting the direction of wave propagation by TOSS; the corresponding circuit diagram of lighting LEDs; the water wave height spectrum extracted from open-circuit voltage by using TOSS; the decomposition diagram of kinetic energy and velocity of ocean waves; the structural analysis diagram of the contact between the hollow buoy and ocean wave; the barycenter distribution of ocean waves in different positions; the short-circuit current spectrum of TOSS by driving the simulative water waves. Supporting Tables 1 and 2 provide the error analysis of wave period extracted by the transferred charges and open-circuit voltage of TOSS (PDF)

AUTHOR INFORMATION

Corresponding Authors

Jie Wang – Beijing Institute of Nanoenergy and Nanosystems, Chinese Academy of Sciences, Beijing 100083, P.R. China;

College of Nanoscience and Technology, University of Chinese Academy of Sciences, Beijing 100049, P.R. China; Center on Nanoenergy Research, School of Physical Science and Technology, Guangxi University, Nanning 530004, P.R. China; orcid.org/0000-0003-4470-6171; Email: wangjie@binn.cas.cn

Zhong Lin Wang – Beijing Institute of Nanoenergy and Nanosystems, Chinese Academy of Sciences, Beijing 100083, P.R. China; School of Materials Science and Engineering, Georgia Institute of Technology, Atlanta, Georgia 30332, United States; Email: zhong.wang@mse.gatech.edu

Authors

Chunguo Zhang – Beijing Institute of Nanoenergy and Nanosystems, Chinese Academy of Sciences, Beijing 100083, P.R. China; College of Nanoscience and Technology, University of Chinese Academy of Sciences, Beijing 100049, P.R. China

Lu Liu – Beijing Institute of Nanoenergy and Nanosystems, Chinese Academy of Sciences, Beijing 100083, P.R. China; College of Nanoscience and Technology, University of Chinese Academy of Sciences, Beijing 100049, P.R. China

Linglin Zhou – Beijing Institute of Nanoenergy and Nanosystems, Chinese Academy of Sciences, Beijing 100083, P.R. China; College of Nanoscience and Technology, University of Chinese Academy of Sciences, Beijing 100049, P.R. China

Xing Yin – Beijing Institute of Nanoenergy and Nanosystems, Chinese Academy of Sciences, Beijing 100083, P.R. China; College of Nanoscience and Technology, University of Chinese Academy of Sciences, Beijing 100049, P.R. China

Xuelian Wei – Beijing Institute of Nanoenergy and Nanosystems, Chinese Academy of Sciences, Beijing 100083, P.R. China

Yue Xiao Hu – Beijing Institute of Nanoenergy and Nanosystems, Chinese Academy of Sciences, Beijing 100083, P.R. China; Center on Nanoenergy Research, School of Physical Science and Technology, Guangxi University, Nanning 530004, P.R. China

Yuebo Liu – Beijing Institute of Nanoenergy and Nanosystems, Chinese Academy of Sciences, Beijing 100083, P.R. China; Center on Nanoenergy Research, School of Physical Science and Technology, Guangxi University, Nanning 530004, P.R. China

Shengyang Chen – Beijing Institute of Nanoenergy and Nanosystems, Chinese Academy of Sciences, Beijing 100083, P.R. China; Center on Nanoenergy Research, School of Physical Science and Technology, Guangxi University, Nanning 530004, P.R. China

Complete contact information is available at: <https://pubs.acs.org/doi/10.1021/acsnano.0c01827>

Author Contributions

[†]These authors contributed equally to this work.

Notes

The authors declare no competing financial interest.

ACKNOWLEDGMENTS

Research was supported by the National Key R&D Project from Minister of Science and Technology (2016YFA0202704), Beijing Municipal Science and Technology Commission (Z171100000317001, Z171100002017017, and Y3993113DF), National Natural Science Foundation of China (grant nos. 61774016, 21773009, 51432005, 5151101243, and 51561145021). Patents have been filed based on the research results presented in this manuscript. The

authors also thank Haining Yu, Jiyuan Zhu, and Liang Lu for this work.

REFERENCES

- (1) Grevenmeyer, I.; Herber, R.; Essen, H. H. Microseismological Evidence for a Changing Wave Climate in the Northeast Atlantic Ocean. *Nature* **2000**, *408*, 349–352.
- (2) Wang, Z. L. New Wave Power. *Nature* **2017**, *542*, 159–160.
- (3) Hristov, T. S.; Miller, S. D.; Friehe, C. A. Dynamical Coupling of Wind and Ocean Waves through Wave-Induced Air Flow. *Nature* **2003**, *422*, 55–58.
- (4) Englander, G. Property Rights and the Protection of Global Marine Resources. *Nat. Sustain.* **2019**, *2*, 981–987.
- (5) Windt, C.; Davidson, J.; Ransley, E. J.; Greaves, D.; Jakobsen, M.; Kramer, M.; Ringwood, J. V. Validation of a CFD-Based Numerical Wave Tank Model for the Power Production Assessment of the Wavestar Ocean Wave Energy Converter. *Renewable Energy* **2020**, *146*, 2499–2516.
- (6) Derie, R. Formaldehyde Oxime Leaching of Metals from Deep-Sea Manganese Nodules and Other Ores. *Nature* **1986**, *324*, 660–661.
- (7) Webb, S. C. The Earth's 'Hum' Is Driven by Ocean Waves over the Continental Shelves. *Nature* **2007**, *445*, 754–756.
- (8) Howell, R.; Walsh, J. Measurement of Ocean Wave Spectra Using a Ship-Mounted HF Radar. *IEEE J. Oceanic Eng.* **1993**, *18*, 306–310.
- (9) Jahn, H.; Oertel, D.; Sandau, R.; Zimmermann, G. Aspects of the Determination of Ocean Wave Parameters by Means of an Optoelectronic Satellite Sensor. *Acta Astronaut.* **1989**, *19*, 513–519.
- (10) Gelpi, C. G.; Schuraytz, B. C.; Husman, M. E. Ocean Wave Height Spectra Computed from High-Altitude, Optical, Infrared Images. *J. Geophys. Res.-Oceans* **2001**, *106*, 31403–31413.
- (11) Sethuraman, S. Momentum Flux and Wave Spectra Measurements from an Air-Sea Interaction Buoy. *Boundary-Layer Meteorol.* **1979**, *16*, 279–291.
- (12) McLean, J. Modeling of Ocean Wave Effects for Lidar Remote Sensing. *Ocean Optics X*; SPIE: Bellingham WA, 1990, Vol. 1302.
- (13) Hwang, P. A.; Teague, W. J.; Jacobs, G. A.; Wang, D. W. A Statistical Comparison of Wind Speed, Wave Height, and Wave Period Derived from Satellite Altimeters and Ocean Buoys in the Gulf of Mexico Region. *J. Geophys. Res.-Oceans* **1998**, *103*, 10451–10468.
- (14) Mouroulis, P.; Van Gorp, B.; Green, R. O.; Dierssen, H.; Wilson, D. W.; Eastwood, M.; Boardman, J.; Gao, B.-C.; Cohen, D.; Franklin, B.; Loya, F.; Lundeen, S.; Mazer, A.; McCubbin, L.; Randall, D.; Richardson, B.; Rodriguez, J. I.; Sarture, C.; Urquiza, E.; Vargas, R.; et al. Portable Remote Imaging Spectrometer Coastal Ocean Sensor: Design, Characteristics, and First Flight Results. *Appl. Opt.* **2014**, *53*, 1363–1380.
- (15) Fan, F.-R.; Tian, Z.-Q.; Wang, Z. L. Flexible Triboelectric Generator! *Nano Energy* **2012**, *1*, 328–334.
- (16) Wang, Z. L.; Jiang, T.; Xu, L. Toward the Blue Energy Dream by Triboelectric Nanogenerator Networks. *Nano Energy* **2017**, *39*, 9–23.
- (17) Chen, J.; Huang, Y.; Zhang, N.; Zou, H.; Liu, R.; Tao, C.; Fan, X.; Wang, Z. L. Micro-Cable Structured Textile for Simultaneously Harvesting Solar and Mechanical Energy. *Nat. Energy* **2016**, *1*, 16138.
- (18) Liang, X.; Jiang, T.; Liu, G.; Feng, Y.; Zhang, C.; Wang, Z. L. Spherical Triboelectric Nanogenerator Integrated with Power Management Module for Harvesting Multidirectional Water Wave Energy. *Energy Environ. Sci.* **2020**, *13*, 277–285.
- (19) Wang, J.; Wen, Z.; Zi, Y.; Zhou, P.; Lin, J.; Guo, H.; Xu, Y.; Wang, Z. L. All-Plastic-Materials Based Self-Charging Power System Composed of Triboelectric Nanogenerators and Supercapacitors. *Adv. Funct. Mater.* **2016**, *26*, 1070–1076.
- (20) Wang, J.; Li, S.; Yi, F.; Zi, Y.; Lin, J.; Wang, X.; Xu, Y.; Wang, Z. L. Sustainably Powering Wearable Electronics Solely by Biomechanical Energy. *Nat. Commun.* **2016**, *7*, 12744.
- (21) Xi, F.; Pang, Y.; Liu, G.; Wang, S.; Li, W.; Zhang, C.; Wang, Z. L. Self-Powered Intelligent Buoy System by Water Wave Energy for Sustainable and Autonomous Wireless Sensing and Data Transmission. *Nano Energy* **2019**, *61*, 1–9.
- (22) Zhang, X.; Zhang, X.; Yu, M.; Ma, Z.; Ouyang, H.; Zou, Y.; Zhang, S. L.; Niu, H.; Pan, X.; Xu, M.; Li, Z.; Wang, Z. L. Self-Powered Distributed Water Level Sensors Based on Liquid-Solid Triboelectric Nanogenerators for Ship Draft Detecting. *Adv. Funct. Mater.* **2019**, *29*, 1900327.
- (23) Wang, J.; Li, X.; Zi, Y.; Wang, S.; Li, Z.; Zheng, L.; Yi, F.; Li, S.; Wang, Z. L. A Flexible Fiber-Based Supercapacitor-Triboelectric-Nanogenerator Power System for Wearable Electronics. *Adv. Mater.* **2015**, *27*, 4830–4836.
- (24) Guo, H.; Pu, X.; Chen, J.; Meng, Y.; Yeh, M.-H.; Liu, G.; Tang, Q.; Chen, B.; Liu, D.; Qi, S.; Wu, C.; Hu, C.; Wang, J.; Wang, Z. L. A Highly Sensitive, Self-Powered Triboelectric Auditory Sensor for Social Robotics and Hearing Aids. *Sci. Robot.* **2018**, *3*, No. eaat2516.
- (25) Zou, Y.; Tan, P.; Shi, B.; Ouyang, H.; Jiang, D.; Liu, Z.; Li, H.; Yu, M.; Wang, C.; Qu, X.; Zhao, L.; Fan, Y.; Wang, Z. L.; Li, Z. A Bionic Stretchable Nanogenerator for Underwater Sensing and Energy Harvesting. *Nat. Commun.* **2019**, *10*, 2695.
- (26) Li, A.; Zi, Y.; Guo, H.; Wang, Z. L.; Fernández, F. M. Triboelectric Nanogenerators for Sensitive Nano-Coulomb Molecular Mass Spectrometry. *Nat. Nanotechnol.* **2017**, *12*, 481–487.
- (27) Xu, M.; Wang, S.; Zhang, S. L.; Ding, W.; Kien, P. T.; Wang, C.; Li, Z.; Pan, X.; Wang, Z. L. A Highly-Sensitive Wave Sensor Based on Liquid-Solid Interfacing Triboelectric Nanogenerator for Smart Marine Equipment. *Nano Energy* **2019**, *57*, 574–580.
- (28) Jing, Q.; Xie, Y.; Zhu, G.; Han, R. P. S.; Wang, Z. L. Self-Powered Thin-Film Motion Vector Sensor. *Nat. Commun.* **2015**, *6*, 8031.
- (29) Isse, T.; Suetsugu, D.; Shiobara, H.; Sugioka, H.; Yoshizawa, K.; Kanazawa, T.; Fukao, Y. Shear Wave Speed Structure Beneath the South Pacific Superswell Using Broadband Data from Ocean Floor and Islands. *Geophys. Res. Lett.* **2006**, *33*, 0094–8276.